

Photon and neutral pion production in pp and Pb-Pb collisions at LHC energies in the ALICE experiment

Podist Kurashvili for the ALICE Collaboration

National Centre for Nuclear Research Warsaw, Poland

(Dated: November 16, 2015)

Abstract

This talk is dedicated to the measurements of direct photons and neutral pions in pp at $\sqrt{s}=2.76$ and 7 TeV and Pb-Pb collisions at $\sqrt{s}=2.76$ TeV per nucleon pair. Photons are measured in the ALICE experiment at mid-rapidity in two electromagnetic calorimeters, Photon Spectrometer (PHOS) and Electromagnetic Calorimeter (EMCal), and via the measurement of the electron-position pairs in the Time Projection Chamber (TPC) and Inner Tracking System (ITS). The latter are produced in the interaction of photons with the material of the detector. Neutral pions are identified via the invariant mass analysis of photon pairs. The combination of different detection methods allows to measure the spectra of particles with high precision over a wide momentum range.

Photons are a unique tool for studying the evolution of nuclear matter produced in the collision as they are emitted during the different stages of the expansion of the initial hot-matter fireball. Photons interact weakly with other particles, escaping almost unchanged and carry information about the properties of the system at the space-time point of their emission.

Direct, high-energy photons, formed at the early stage of the collision, provide a test of perturbative QCD, set constraints on the parton distribution and fragmentation functions and determine the initial energy of jets produced by high-energy quarks. Thermal photons result from interactions of particles in both hot QGP and cooler Hadron Gas phases, and carry information about the temperature of the medium. The spectra of photons and the effective temperature extracted from the thermal photon yield will be presented and compared with the results of the PHENIX experiment.

The measurement of neutral pion yields permits a study of medium-induced energy loss via the transverse momentum dependence of the nuclear modification factor R_{AA} , expressing the modification of π^0 p_T -spectra in Pb-Pb collisions with respect to pp interactions, as a function of collision centrality.

INTRODUCTION

The quark-gluon plasma (QGP) is the state of matter at high temperature characterized by deconfinement of quarks and gluons [1]. The QGP could have existed in the early hot Universe up to about 10^{-6} s after the Big Bang. After expansion and cooling, quarks and gluons were confined into hadrons which we observe in ordinary matter. Present-day heavy-ion experiments try to produce extremely hot matter with vanishing baryon density by colliding heavy ions, which would lead to a temperature above the quark-gluon plasma transition point $T \sim 155$ MeV [2] ("little Big Bang"). The hot matter fireball formed in the collision undergoes subsequent expansion going through the quark-gluon plasma and hadron gas stages and ends by freeze-out when the final-state particles stream freely out of the reaction zone.

The measurement of direct photons is one of the most interesting challenges in exploring the quark-gluon plasma. Direct photons can be divided in two groups according to the mechanism of emission. *Prompt* photons are produced in the initial parton interactions and dominate the high- p_T part of the direct photon spectrum. *Thermal* photons are formed in secondary interactions between quarks and gluons in the hot matter fireball with energy far below that of original interactions. Photons experience a very weak interaction with the matter and escape almost unperturbed from the reaction zone carrying information about the thermal and dynamical properties of the medium at the point of their emission.

Decay photons, which constitute the major part of the photon spectrum, help to reconstruct short-lived particles, such as neutral pions that have the dominant two-photon decay channel. Neutral pions are produced by quark and gluon fragmentation in the initial high-energy collisions (hard part) and from the quark-gluon matter fireball (soft part). Unlike the direct photon case, their production is highly affected by the medium. The study of in-medium modification of the neutral pion yield and π^0 -hadron correlations probes the stopping power of the hot matter.

Measurement of direct photons in pp and p-Pb collisions helps to build a reference for studying the properties of matter in Pb-Pb collisions. These measurements also provide a tool to probe the perturbative regime of Quantum Chromodynamics and tests the validity of the initial parton distributions and fragmentation functions used in current particle generators.

In this talk we present results obtained in the ALICE LHC experiment during the Run 1 in 2010-2011 for proton-proton and lead-lead interactions at 0.9, 2.76 and 7 TeV.

PHOTON MEASUREMENTS IN ALICE

The ALICE experiment is a dedicated heavy-ion experiment designed to study the quark-gluon plasma and one of four major experiments at the Large Hadron Collider (LHC) at CERN. The ALICE detector system is designed to cope with the high multiplicities of final state particles in the mid-rapidity region and combines different techniques of measurement for different kinds of particles. The ALICE experiment is the only LHC experiment with the capability to measure and identify particles with low p_T ($\leq 1 \text{ GeV}/c$). The full description of the experimental setup and techniques used in measurements can be found in [3]. Below we shall concentrate on photon detection with detectors highlighted in Figure 1.

There are two methods of photon measurements used in the ALICE experiment. The first, called photon conversion method (PCM), is based on detecting photons by their conversions to electron-positron pairs in the material of the detectors. Electron-positron pairs are reconstructed in the tracking detectors, ITS consisting of six layers of silicon detectors and gaseous TPC. The experimental setup provides high acceptance for this method (full azimuthal angle, $|\eta| < 0.9$), although the probability of the photon conversion is rather low ($\sim 8.5\%$) due to the small material budget of the detectors. The PCM is characterized by high precision of energy measurement at low transverse momenta, $p_T \leq 1 \text{ GeV}/c$.

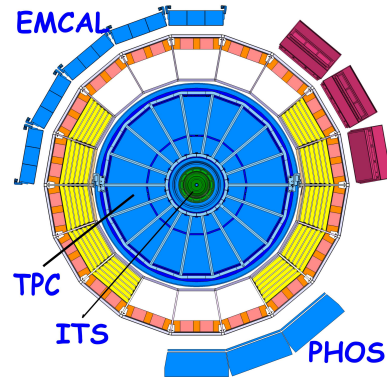


FIG. 1: ALICE detectors used in detection of photons.

Another method is based on calorimetry. Two calorimeters, PHOS and EMCal, are designed for high precision photon measurements over a wide dynamical range. The three PHOS modules consist of 10752 PbWO_4 crystals with $2.2 \times 2.2 \text{ cm}^2$ cross section and 18 cm depth, corresponding to approximately 20 radiation lengths. The acceptance of PHOS is $|\eta| < 0.12$ and 60 degrees of azimuthal angle. Its high granularity and excellent energy resolution allow the detection of photon pairs from π^0 decays at high p_T . Good time resolution makes possible the application of a time-of-flight filter.

The EMCal consists of Pb-scintillator sandwich layers with cell of transverse size $6 \times 6 \text{ cm}^2$ and depth 24.6 cm, which also makes up about 20 radiation lengths. Its acceptance is $|\eta| < 0.7$

and 107 degrees of azimuthal angle.

NEUTRAL PIONS IN pp AND Pb–Pb COLLISIONS

Neutral pions are extracted using an invariant mass analysis, combining all possible pairs of reconstructed photons and calculating the mass of the pairs:

$$M_{inv}^2 = (p_1 + p_2)^2 = 2\epsilon_1\epsilon_2(1 - \cos\theta_{12}), \quad (1)$$

where, $p_{1,2}$, $\epsilon_{1,2}$ are the four-momenta and energies of the two photons, respectively and θ_{12} is their opening angle.

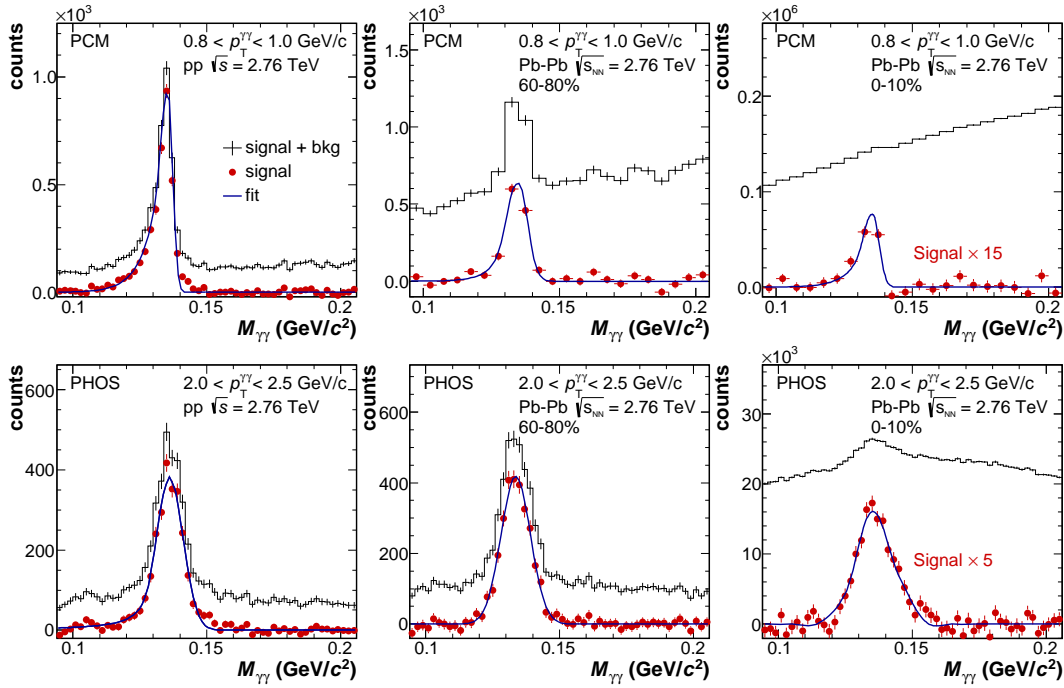


FIG. 2: Invariant mass spectra in selected p_T slices for PCM (upper row) and PHOS (lower row) in the π^0 mass region for pp (left column), 60 – 80% centrality Pb–Pb collisions (middle column) and 0 – 10% centrality (right column) Pb–Pb collisions [4]. The histogram and the filled points show the data before and after background subtraction, respectively. For the 0 – 10% class the invariant mass distributions after background subtraction were scaled by a factor 15 and 5 for PCM and PHOS, respectively, for better visibility of the peak. The positions and widths of the π^0 peaks were determined from the fits to the invariant mass spectra after background subtraction (blue curves).

The resulting M_{inv} distribution is peaked near $m_{\pi^0}=0.135 \text{ GeV}/c^2$ and also contains combinatorial background, as shown in several examples in Figure 2. The event mixing technique was used for precise evaluation and subtraction of the background [4]. As one can see, the extraction method works both in low and high multiplicity environments.

The raw π^0 spectrum obtained from the invariant mass analysis is corrected for detector acceptance and efficiency in order to determine the production cross section. Figure 3 represents the comparison of results obtained from PCM and calorimetric (PHOS) measurements in the case of Pb–Pb collisions, where both histograms are divided by the function fitting the combined p_T -distribution. The results obtained by the two methods agree within errors.

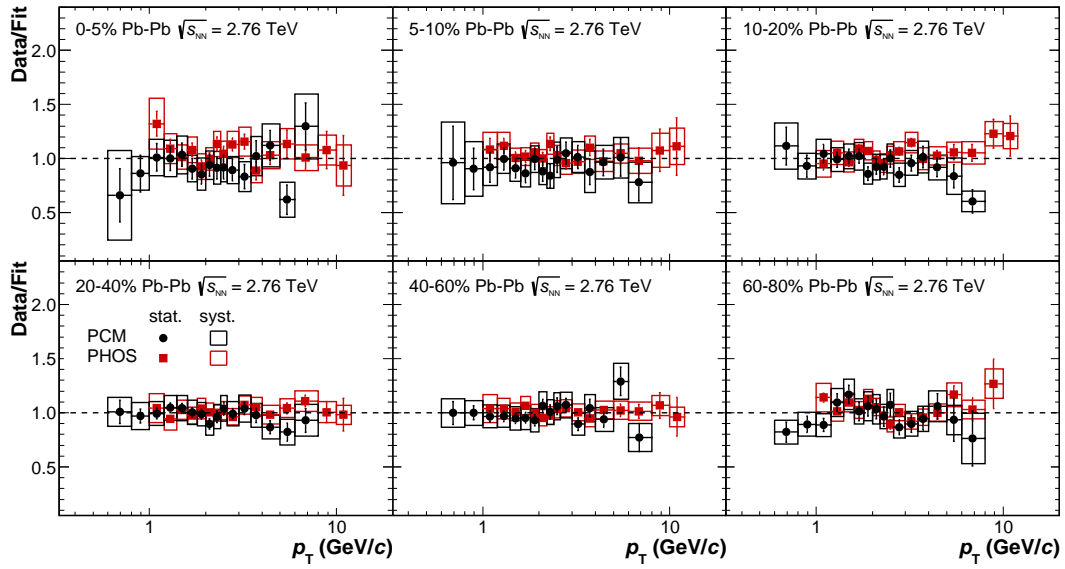


FIG. 3: Ratio of the fully corrected π^0 spectra in Pb-Pb collisions at $\sqrt{s_{NN}} = 2.76$ TeV in six centrality bins measured with PHOS and PCM to the fits to the combined result in each bin [4]. Vertical lines represent statistical uncertainties, the boxes are the systematic uncertainties.

The neutral pion production cross section is plotted in Figure 4 for three different collision energies, 0.9, 2.76 and 7 TeV. The comparison to Next to Leading Order (NLO) perturbative QCD calculation shows a good agreement between theory and experiments at $\sqrt{s} = 0.9$ TeV. At 2.76 and 7 TeV, theory overestimates the π^0 production cross section. This may be connected to the imprecise knowledge of the gluon fragmentation functions, which are not well defined by existing data at low \sqrt{s} [6].

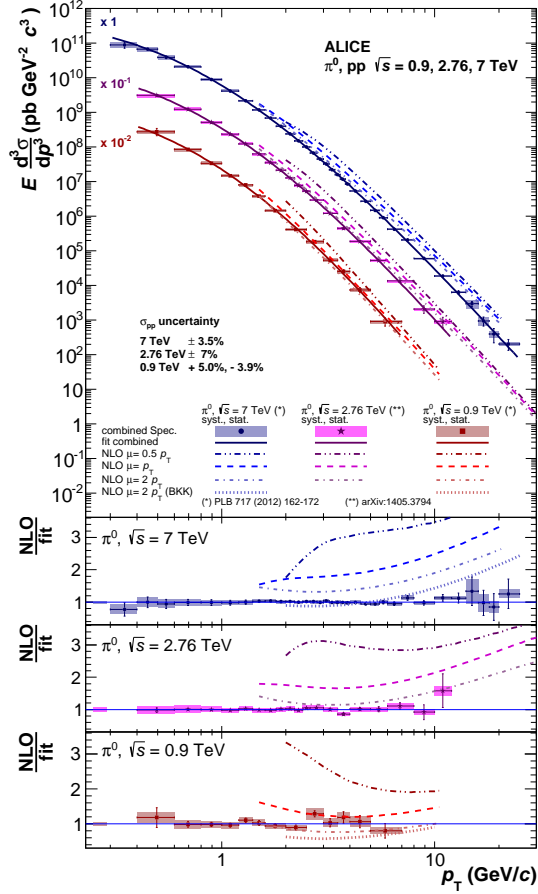


FIG. 4: Differential cross section of π^0 production in pp collisions at $\sqrt{s} = 0.9, 2.76$ and 7 TeV [5]. NLO pQCD calculations for three factorization scales $\mu_F = 0.5p_T, p_T, 2p_T$ are shown.

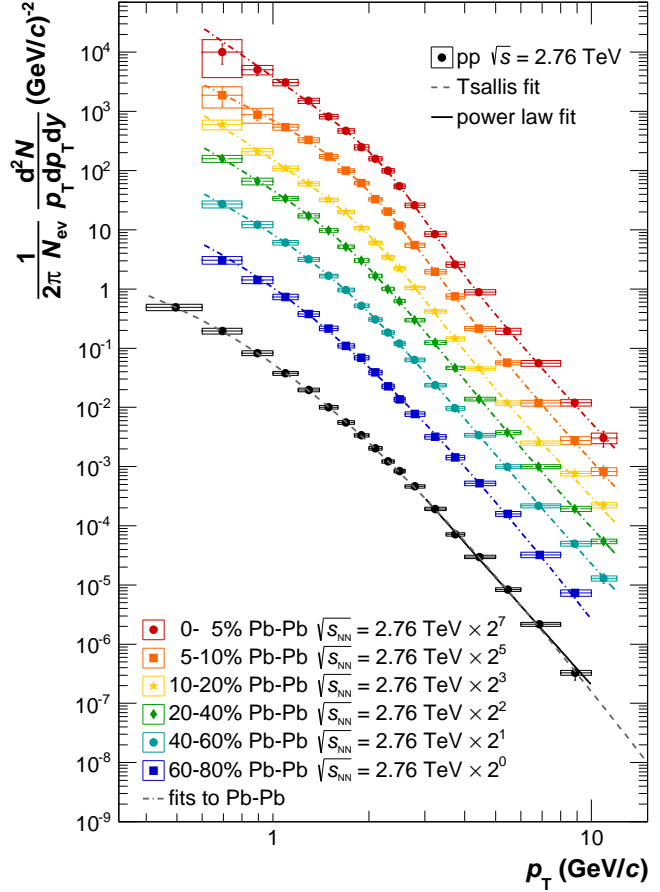


FIG. 5: Invariant differential yields of neutral pions produced in Pb–Pb and inelastic pp collisions at $\sqrt{s_{NN}} = 2.76$ TeV [4]. The spectra are the weighted average of the PHOS and the PCM results.

The results for Pb–Pb invariant yields are shown in Figure 5. Comparison of these results to the pp yield gives the nuclear modification factor, R_{AA} :

$$R_{AA}(p_T) = \frac{\frac{d^2 N}{dp_T dy}|_{AA}}{\langle T_{AA} \rangle \times \frac{d^2 \sigma}{dp_T dy}|_{pp}}. \quad (2)$$

R_{AA} measures the ratio of the π^0 yield in Pb–Pb collisions compared to the yield in pp collisions scaled by the number of binary nucleon-nucleon collisions in a specified centrality range, $N_{coll} = \langle T_{AA} \rangle \sigma_{inel}^{pp}$. A deviation of R_{AA} below unity represents a suppression of π^0 production in Pb–Pb collisions.

Figure 6 shows R_{AA} calculated for three bins of collision centrality. Pion production is most suppressed in central Pb–Pb collisions. The modification factor levels off at $p_T > 4$ GeV/ c and is equal to 0.1 for most central collisions which is two times lower than the result obtained by the

PHENIX experiment at RHIC [7], which indicates a larger energy loss compared to RHIC. Below 4 GeV/ c the spectrum is dominated by soft QCD processes in the medium and boosted by flow, resulting in growth of R_{AA} at small p_T .

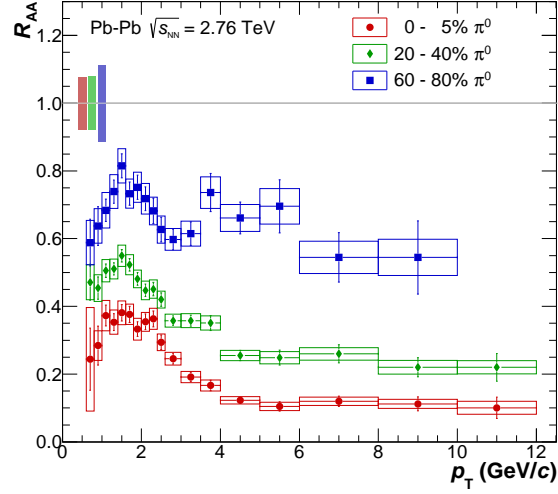


FIG. 6: Neutral pion nuclear modification factor R_{AA} for three different centralities (0-5%, 20-40%, 60-80%) in Pb-Pb collisions at $\sqrt{s_{NN}} = 2.76$ TeV [4]. The boxes around unity reflect the uncertainty of the average nuclear overlap function $\langle T_{AA} \rangle$ and the normalization uncertainty of the pp spectrum added in quadratures.

NEUTRAL PION ANGULAR CORRELATIONS

High transverse momentum quarks and gluons produced in the collisions hadronize creating a spray of hadrons emitted in narrow cones around the direction of the scattered partons called jets. A jet is commonly accompanied by another parton flying in opposite direction. Two opposite jets produced in quark-gluon plasma should undergo different degree of suppression if their paths in medium are different. In π^0 -hadron correlation measurements, pions with high p_T are presumed to be the leading particle of hadron jets produced near the surface of quark-gluon plasma. In that case, the jet of the corresponding recoil particle should be observed in the opposite direction as is shown in Figure 7.

We looked for correlations between these pions, which were taken as trigger particles, and charged hadrons (associated particles) by studying the azimuthal angle $\Delta\varphi = \varphi^{trig} - \varphi^{assoc}$. Charged hadrons were detected by the tracking detectors and pions were measured with EM-CAL using a combination of invariant mass and cluster shape analyses.

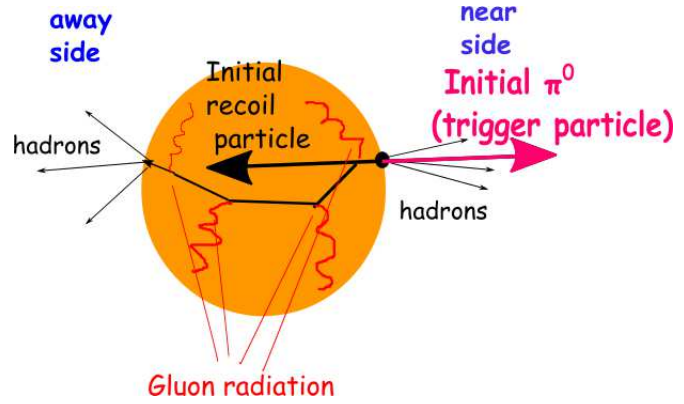


FIG. 7: Graphical representation of trigger π^0 , associated hadrons and near and away sides.

The latter is based on the difference of the second moment of the cell energy distribution in the cluster. The greater eigenvalue of this tensor significantly varies depending on whether a cluster was produced by a single photon or by a closely separated pair of photons from π^0 decay.

Defining the charged hadron yield per trigger particle, $Y^{pp}(p_T^{\pi^0}, p_T^{h^\pm})$ and $Y^{AA}(p_T^{\pi^0}, p_T^{h^\pm})$, for pp and Pb–Pb collisions, respectively, the observable that quantifies medium effects is the modification factor:

$$I_{AA}(p_T^{\pi^0}, p_T^{h^\pm}) = \frac{Y^{AA}(p_T^{\pi^0}, p_T^{h^\pm})}{Y^{pp}(p_T^{\pi^0}, p_T^{h^\pm})} \quad (3)$$

The results for correlations for pp and Pb–Pb collisions are presented in Figure 8. As one can see, there are two maxima close to $\Delta\varphi = 0$ (near side) and $\Delta\varphi = \pi$ (away side) in pp collisions.

The modification factor at near and away sides is presented in Figure 9. The away-side

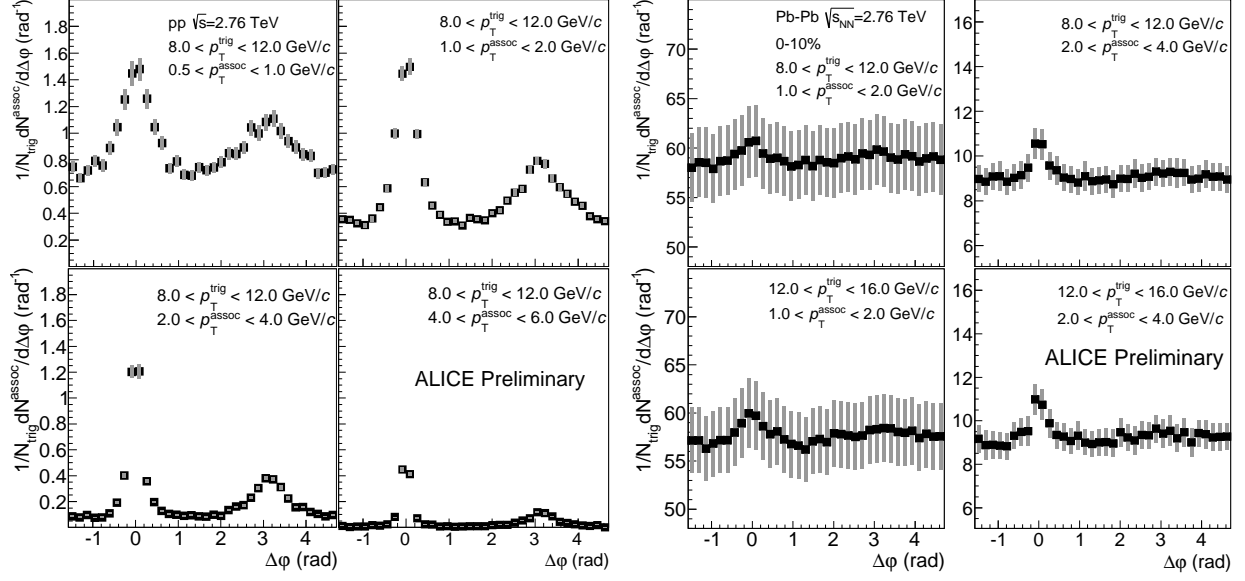


FIG. 8: Azimuthal angle distribution of π^0 -hadron correlations for different bins of transverse momentum of associated particles with the trigger π^0 in p_T bins 8-12 GeV/c for pp collisions at $\sqrt{s}=2.76$ TeV (left) and 8-12 GeV/c and 12-16 GeV/c for Pb-Pb collisions at $\sqrt{s_{NN}}=2.76$ TeV, centrality 0-10% (right).

correlation exhibits suppression by a factor of two due to energy loss in the medium. The near-side enhancement by about 20% can be explained by several factors, such as a change of the fragmentation function, different fractions of quark and gluon jets in the medium compared to the pp case, and bias of parton p_T distribution due to in-medium energy loss [8].

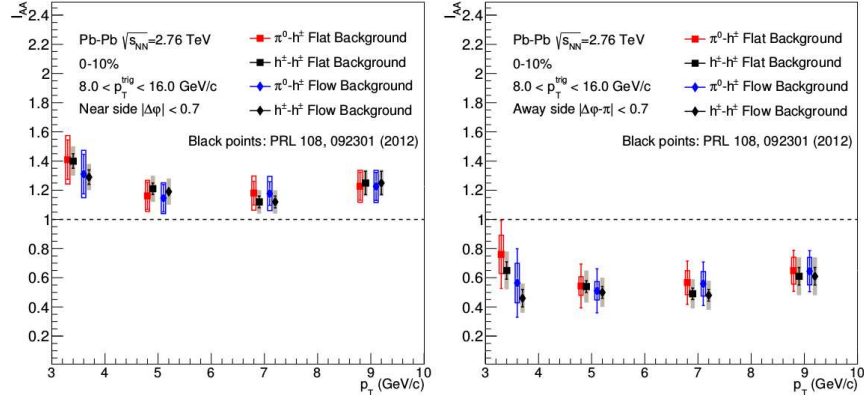


FIG. 9: Modification of per-trigger yield of charged hadrons, I_{AA} , on the near (left) and away (right) side for π^0 -hadron correlations at 0-10% in Pb-Pb collisions at $\sqrt{s_{NN}}=2.76$ TeV.

DIRECT PHOTONS

Direct photons are defined as those which do not originate from decay of unstable particles:

$$\gamma_{\text{direct}} = \gamma_{\text{inc}} - \gamma_{\text{decay}} = \gamma_{\text{inc}} \cdot \left(1 - \frac{\gamma_{\text{decay}}}{\gamma_{\text{inc}}}\right) = \gamma_{\text{inc}} \cdot \left(1 - \frac{1}{R}\right), \quad (4)$$

where γ_{inc} and γ_{decay} denote inclusive and decay photon spectra, respectively, their ratio is $R = \gamma_{\text{inc}}/\gamma_{\text{decay}}$. $R > 1$ signals the presence of direct photons.

In our analysis, we used a double ratio:

$$R_\gamma = \frac{\gamma_{\text{inc}}/\pi_{\text{meas}}^0}{\gamma_{\text{decay}}/\pi_{\text{param}}^0} \approx R, \quad (5)$$

where π_{meas}^0 is the measured π^0 spectrum and π_{param}^0 is its fitting function. The advantage of this method is that major systematic uncertainties, associated with photon and π^0 measurement, cancel in the ratio. The measured double ratio for pp and Pb–Pb collisions is plotted in Figures 10 and 11 along with the Next to Leading Order (NLO) perturbative QCD predictions. R_γ for pp collisions is found to be in agreement with the NLO pQCD calculations (left hand side of Figure 10). The same agreement is observed for double ratio in peripheral (40-80%) Pb–Pb collisions (right hand side of Figure 10), whereas the result for central (0-40%) Pb–Pb exhibits significant excess above the pQCD prediction at $p_T < 4$ GeV/c, as shown in Figure 11.

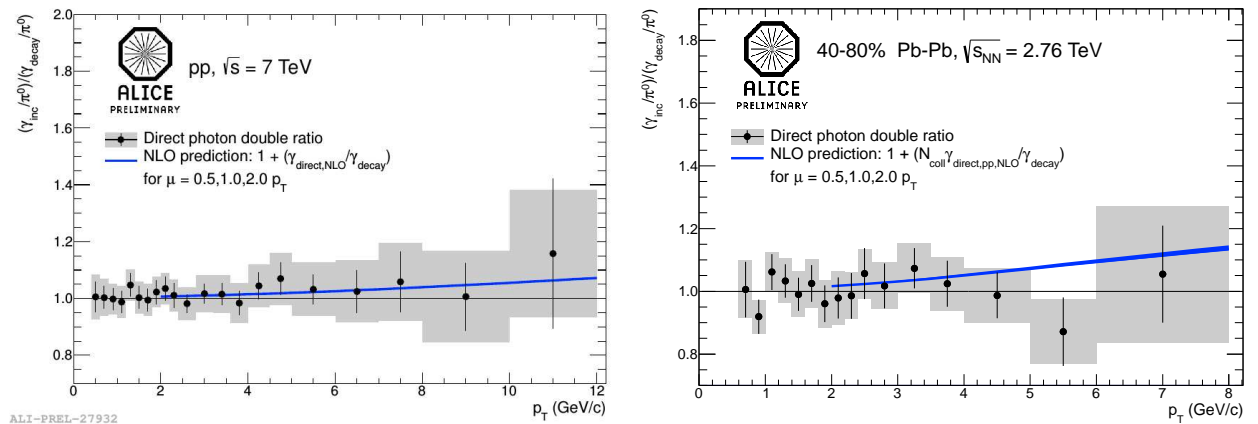


FIG. 10: Direct photon double ratio and NLO pQCD prediction (blue curve) in pp collisions at $\sqrt{s} = 7$ TeV (left) and at 40-80% in Pb–Pb collisions at $\sqrt{s_{NN}} = 2.76$ TeV (right) [9]. The spread of the blue curve corresponds to different factorization scales $\mu_F = 0.5p_T, p_T, 2p_T$.

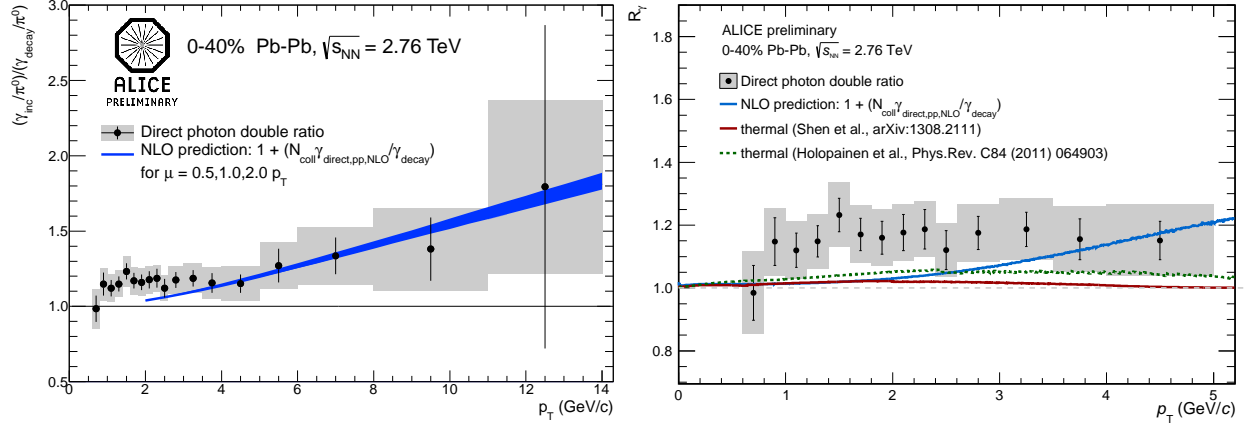


FIG. 11: Direct photon double ratio with NLO pQCD at centrality 0-40% in Pb-Pb collisions at $\sqrt{s_{NN}} = 2.76$ TeV [9] (left). Measured double ratio with that predicted by hydrodynamic models (right).

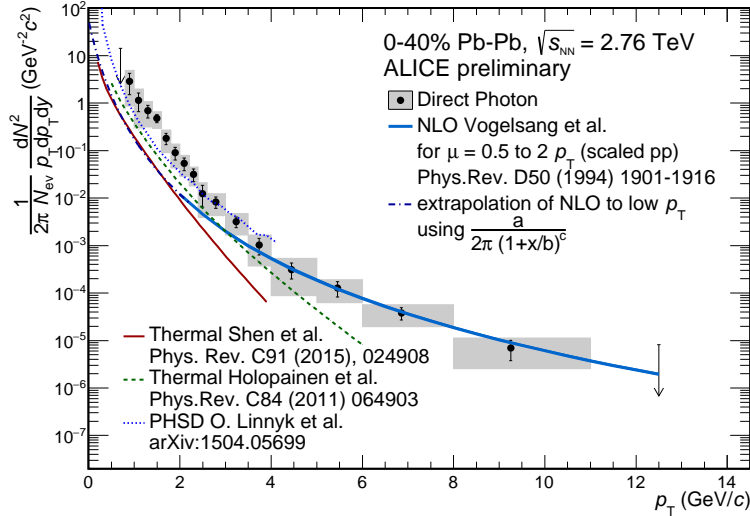


FIG. 12: Direct photon spectrum at 0-40% in Pb-Pb at 2.76 TeV with NLO pQCD calculation and hydrodynamic model predictions.

The right hand side of Figure 11 depicts the excess at $p_T \leq 5$ GeV/c in more detail. The measured double ratio exceeds that predicted by hydrodynamic models. The invariant yield of direct photons is plotted in Figure 12. An exponential fit of the direct photon spectrum of the form $A \cdot \exp(-p_T/T_{\text{eff}})$ for $p_T \leq 2.2$ GeV/c yields an estimate for the inverse slope of the exponent:

$$T_{\text{eff}} = 304 \pm 51^{\text{stat}+\text{sys}} \text{ MeV}.$$

The obtained value of T_{eff} is larger than the result obtained by the PHENIX experiment, $T_{\text{eff}}^{\text{RHIC}} = 219 \pm 19^{\text{stat}} \pm 19^{\text{sys}} \text{ MeV}$ at $\sqrt{s_{NN}} = 200$ GeV [10]. T_{eff} reflects the average temperature

of matter during its evolution but is also affected by flow [11]. A consistent interpretation of T_{eff} in terms of the temperature requires the understanding of the evolution of the fireball.

The initial spatial anisotropy of non-central ion-ion collision leads to the build-up of collective anisotropic flow, which is described in the distribution of final state particles as a function of azimuthal angle φ :

$$\frac{dN}{d\varphi} = \frac{N}{2\pi} \cdot \left(1 + \sum_{n>1} v_n \cos(n[\varphi - \Psi_R]) \right), \quad (6)$$

where Ψ_R is the orientation of the reaction plane as shown in Figure 13.

The thermal photons are expected to be produced at an early phase of the collision and measurement of their flow will help us to understand development of the collective expansion at early times. Experimentally, one can measure the flow of inclusive photons, estimate the flow of decay photons and calculate the direct photon flow from the following expression:

$$v_n^{\text{direct}} = \frac{R_\gamma \cdot v_n^{\text{inc}} - v_n^{\text{decay}}}{R_\gamma - 1}. \quad (7)$$

Figure 14 represents the v_2 coefficient measuring elliptic flow for inclusive and decay photons. The elliptic flow of direct photons presented in Figure 15 is non-zero in the same p_T interval where the excess of the yield over the perturbative QCD prediction was observed.

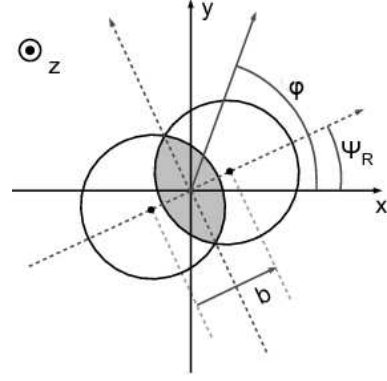


FIG. 13: Schematic view of a non-central ion-ion collision with non-zero impact parameter b . The direction of the line connecting the centres of the colliding nuclei defines the orientation of the reaction plane expressed by the angle Ψ_R used in (6).

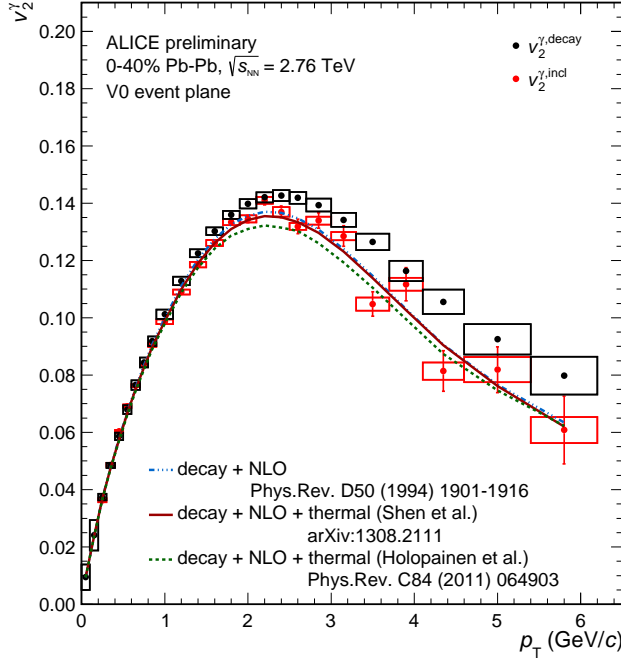


FIG. 14: Comparison of elliptic flow of inclusive and decay photons in 0-40% Pb-Pb collisions at 2.76 TeV with theory.

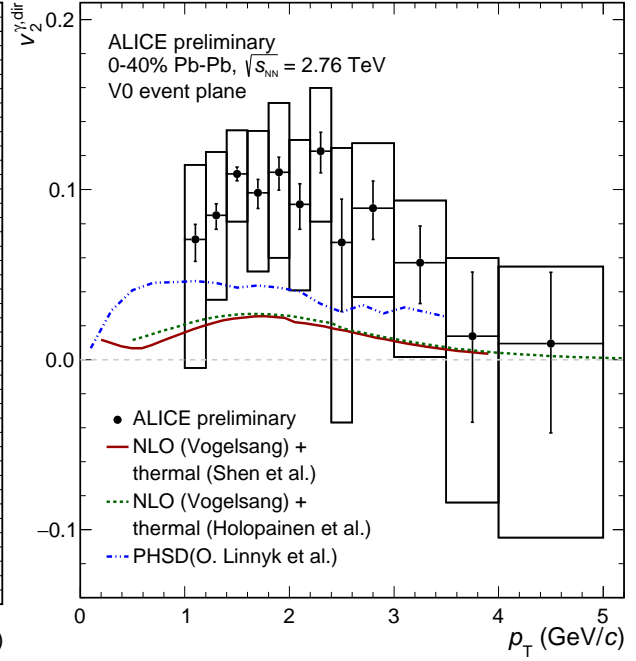


FIG. 15: Elliptic flow of direct photon measured in experiment with theory.

SUMMARY

We have presented the results of direct photon and π^0 production obtained from proton-proton and lead-lead collisions in the ALICE experiment. Measurement of neutral pions in pp collisions allowed to test the validity of QCD-inspired models. The QCD predictions agree with the measurements at $\sqrt{s} = 0.9$ TeV but overpredict pion yields at higher collision energies.

The nuclear modification factor for neutral pions demonstrates a suppression of the pion yield by factor 10 for the most central collisions with respect to scaled pp collisions at the same energy.

The study of jet-like, π^0 -hadron correlations reveals a strong away side suppression and smaller near side enhancement in Pb-Pb collisions due to in-medium effects.

An excess of direct photons was found in Pb-Pb collisions over that predicted from pQCD calculations and hydrodynamical models. The effective temperature was found to be $T_{\text{eff}} = 304 \pm 51^{\text{stat+sys}} \text{ MeV}$. A non-zero elliptic flow of direct photons was observed within the same p_T interval as the excess of thermal photons.

-
- [1] S. Borsanyi et al., JHEP **077**, 1011 (2010).
 - [2] G. Martinez, arXiv:1304.1452.
 - [3] K. Aamodt et al., J. of Instr. **S08002**, 3 (2008).
 - [4] B. Abelev et al., Eur.Phys.J. **C74**, 3108 (2014).
 - [5] B. Abelev et al., Phys.Lett. **B717**, 162-172 (2012).
 - [6] D. de Florian et al., arXiv:1410.6027 (2014).
 - [7] S. Adler et al., Phys.Rev.Lett. **C76**, 034904 (2007).
 - [8] K. Aamodt et al., PRL **108**, 092301 (2012)
 - [9] M. Wilde, Nucl.Phys. **A904**, 573 (2013).
 - [10] A. Adare et al., Phys.Rev.Lett. **109**, 122302 (2012).
 - [11] S. Chen, U. Heinz, Phys.Rev. **C89**, 4, 044910, (2014).